Preparation and Properties of Polyurethane/Benzyl Amylose Semi-Interpenetrating Networks

Xiaodong Cao,[1,2] Yongzhen Tao,[1] Lucian A. Lucia,[2] Lina Zhang[1]

[1]*Department of Chemistry, Wuhan University, Wuhan 430072, China*
[2]*Department of Wood and Paper Science, North Carolina State University, Raleigh, North Carolina 27695-8005*

Received 15 June 2009; accepted 27 September 2009
DOI 10.1002/app.31497
Published online 23 December 2009 in Wiley InterScience (www.interscience.wiley.com).

ABSTRACT: A series of semi-interpenetrating polymer networks (semi-IPNs) films were prepared from 20 wt % of benzyl amylose (BA) of different M_w and castor oil-based polyurethane (PU) in *N,N*-dimethylformamide (DMF). The weight-average molecular weight (M_w), and radii of gyration ($<S^2>_z^{1/2}$) of benzyl amylose were determined by laser scattering measurement, and the results suggested BA was in a compact coil conformation in DMF. Furthermore, the properties and miscibility of the polyurethane/benzyl amylose (PUBA) films were studied by scanning electronic microscopy, differential scanning calorimetry, dynamic mechanical thermal analysis, ultraviolet–visible spectrophotometer, and tensile testing. The PUBA films possessed much higher optical transmittance and tensile strength than the pure PU film regardless of the molecular weight of BA, but lower values of elongation at break were observed. With decreasing of the BA M_w from 9.24×10^5 to 2.69×10^5, interestingly, the elongation at break of the films increased from 135 to 326%. This might be ascribed to the decrease of crosslinking density of PU networks and the enhancement in freedom of the molecular motion. © 2009 Wiley Periodicals, Inc. J Appl Polym Sci 116: 1299–1305, 2010

Key words: benzyl amylose; molecular weight; miscibility; properties

INTRODUCTION

The study and application of polymers from renewable resources has received increased attention over the last two decades.[1–4] Several highly competitive advantages of renewable polymeric starting materials for specific end-use applications include their low cost, ready availability, renewability, and biodegradability.[5] Starch, one of the most abundant renewable polymers in the world, is among the most promising starting materials. It usually has two major components, namely, largely linear amylose groups having a relatively low molecular weight, consisting of α-(1→4)-linked D-glucose, and amylopectin groups having the same backbone as amylase, but with a myriad of α-(1→6)-linked branch points. However, starch is mostly water soluble, difficult to process, brittle, and has poor mechanical properties. To address these shortcomings, various physical or chemical modifications of starch have been considered, including blending,[6] chemical derivation,[7] and graft copolymerization.[8]

Vegetable oils are predominantly made up of triglyceride molecules, a chemical feature that allows them to be considered for (bio)-diesel production. They offer a valuable substitute polymer feedstock relative to petroleum because they are renewable, easily processed, biodegradable, and offer comparable performance and cost.[9–13] Among all the vegetable oils, castor oil is the only major oil composed essentially of the triglycerides of a hydroxyl acid, ricinoleic acid, that makes it one of the most important commercial oils.[14] Polyurethane (PU) prepared from castor oil is a useful, versatile material that is widely used as an individual processing network structure because of its good flexibility and elasticity. In our laboratory, a series of semi-interpenetrating network (semi-IPN) materials from castor oil-based PUs and different types of natural polymers as well as their derivatives have been successfully prepared, such as PU/nitrocellulose,[15] PU/nitrokonjac glucomannan,[16] and PU/benzyl konjac glucomannan.[17,18] The results indicated that the incorporation of the natural polymers into PU not only accelerates the curing process but also enhances the biodegradability of the semi-IPN materials. Moreover, the PU/natural polymer semi-IPN materials

Correspondence to: L. A. Lucia (lucian.lucia@ncsu.edu) or L. Zhang (lnzhang@public.wh.hb.cn).

Contract grant sponsor: National Natural Science Foundation of China; contract grant numbers: 59933070, 30530850.

Contract grant sponsor: National Sciences Foundation of China; contract grant number: 20474048.

Contract grant sponsor: Laboratory of Cellulose and Lignocellulosic Chemistry of the Chinese Academy of Sciences.

can be degraded by microorganisms in soil accompanied with production of CO_2, H_2O, and aromatic ethers.[19]

Recently, we synthesized a starch derivative, benzyl starch (BS) to prepare PU/BS semi-IPNs.[20] It is worth noting that the semi-IPN material, PU/BS shows a specific degree of miscibility and good mechanical properties when the concentration of BS component ranged from 5 to 70 wt %. The effect of molecular weight of BS on the properties of PU/BS has been studied and the results indicated that the PU/BS containing low M_w BS has better miscibility and mechanical properties.[21] However, the BS with a M_w lower than 1 million was not well investigated because the amylopectin component of starch has too high of a M_w. In this work, therefore, we synthesized a series of benzyl amylose (BA) compounds with M_ws lower than 1 million from pure corn amylose. The values of M_w and intrinsic viscosity ([η]) of BA in *N,N*-dimethylformamide (DMF) and were determined by light scattering and viscometry, respectively, and the chain conformation was evaluated based on current polymer solution theories. Subsequently, a series of semi-IPN materials from castor oil-based PU and BA with different M_ws were prepared by solution casting. The effect of the M_w of BA on the structure and properties of the resultant semi-IPN materials was studied.

EXPERIMENTAL

Materials

Corn amylose was supplied by Wako Pure Chemical Industries and used as received. 4,4′-diphenylmethane diisocynate (MDI) was purchased from Aldrich and used as received. Castor oil (a chemical reagent with a 4.49 wt % content of hydroxyl groups and hydroxyl value of 163) was dried at 110°C under 20 mmHg for 2 h. *N,N*-dimethylformamide (DMF) and dimethyl sulfoxide (DMSO) were dried over molecular sieves (4 Å) for 1 week before use.

Preparation of BA fractions

A total of 8 g of amylose was introduced into 100 mL of 20 wt % sulfuric acid aqueous solutions at room temperature and stirred for a prescribed time, and the suspension was then filtered and washed with distilled water until the pH = 7. Then, the product was dispersed in 100 mL of water and introduced into a three-necked bottom flask equipped with a mechanical stirrer, a funnel, a condenser, into which 40 g of 35 wt % sodium hydroxide aqueous solution was added. The resultant alkali–starch slurry was stirred at 40°C for 30 min before 20 g of

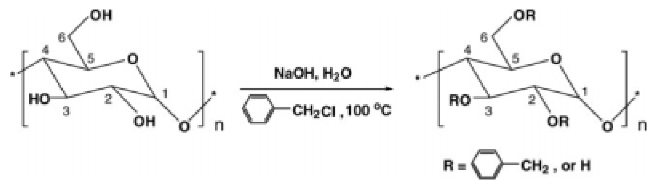

Scheme 1 Synthesis of benzyl amylose.

benzyl chloride was added dropwise. The benzylation reaction was performed at ∼100°C for 1 h to obtain a white precipitate (Scheme 1). Subsequently, the precipitate was washed with acetone and water successively over five times and dried in vacuum at room temperature. By adjusting the exposure time of amylose to sulfuric acid aqueous solution for 0, 1, 3, 5, and 7 h, a series of BA products with different M_w values were obtained and coded as BA0, BA1, BA3, BA5, and BA7, respectively.

Preparation of PUBA

A four-necked flask was fitted with a nitrogen inlet tube, a mechanical stirrer, thermometer, and a pressure-equalizing dropping funnel. A total of 50 g of MDI were poured into flask and then heated for melting at 40°C. Into the flask under a nitrogen atmosphere with dropping were added 69 g of castor oil. The dropping was completed within 50 min. Then, the stirring was maintained 2 h to get the PU prepolymer ([NCO]/[OH] = 2). PU prepolymer, 20 wt % BA, and 1,4-butanediol as a chain extender (the samount was adjusted to give a total [NCO]/[OH] = 1) were dissolved in DMF and mixed at room temperature. The resultant mixture had a solid content of about 10 wt % and was cast onto a glass plate and dried at 60°C for 12 h to obtain transparent PUBA semi-IPN films. The PUBA films having thicknesses of ∼200 μm were subsequently peeled off and coded as PUBA0, PUBA1, PUBA3, PUBA5, and PUBA7, respectively, corresponding to the code of BA. As a control, the PU film without the addition of BA was prepared using the same process. However, it required ∼24 h to obtain a dry film, which was much longer than that used for the PUBA films. All the resulting films were vacuum-dried at room temperature for 3 days and kept in a desiccator with P_2O_5 as desiccant for more than 1 week before characterization.

Light scattering measurement

The light-scattering intensities of the BA samples in DMF were determined with a multiangle laser light scattering (LLS) instrument equipped with a He-Ne laser (λ = 632.8 nm, DAWN®DSP, Wyatt Technology Co.) at angles of 40, 55, 62, 71, 80, 90, 100, 109, 119, and 138 at 25°C. Sample solutions of desired concentration were prepared, and optical clarity was achieved by filtration through a sand filter followed by 0.45 μm filter (Whatman) in the cell (SV mode). The refractive index increment (dn/dc) of BA in DMF was measured with a double-beam differential refractometer (DRM-1020, Otsuka Electronics Co.) at 633 nm and 25°C. The dn/dc value was determined to be 0.162 mL g^{-1}. Astra software was used to collect the signal and analyze the data to obtain M_w and $<S^2>_z^{1/2}$ according to the following equation:

$$(Kc/R_\theta)^{1/2} = (1/M_w{}^{1/2})[1 + (1/6) <S^2>_z q^2 + M_w A_2 c] \tag{1}$$

where $K = (2\pi^2 n^2/N_A\lambda^4)(dn/dc)^2$, $q = (4\pi n/\lambda)\sin(\theta/2)$, N_A is Avogadro's number, λ is the wavelength of incident light in a vacuum, and n is the refractive index of solution.

Characterization

The degree of substitution (DS) indicates the average number of substitutions per anhydroglucose unit. There are three free hydroxyl groups available for modification, resulting in a maximum possible DS = 3. As shown in Scheme 1, when substituting the benzyl groups for the H atom of hydroxyl on the anhydroglucose unit, the content of the carbon of BA was changed. Therefore, the DS values of BA may be calculated by

$$\mathrm{DS} = \frac{162w_c - 72}{84 - 90w_c} \tag{2}$$

where w_c is the content of carbon of BA obtained from element analysis, which was carried out on a elemental analyzer (CHN-O-RAPID Heraeus).

Scanning electron microscopy (SEM) images were taken on a SEM microscope (Hitachi S-570). The PUBA films were frozen in liquid nitrogen and split immediately, and the cross-sections of the films were coated with gold for SEM observation. SEM images were examined at an accelerating voltage of 20 kV.

Differential scanning calorimetry (DSC) measurements of BA0 and PUBA films were carried out on a DSC apparatus (200 PC, Netzsch) under a nitrogen atmosphere at a heating rate of 20°C min^{-1} from −50 to 200°C. Before the test, the samples (ca.10 ± 1 mg) were heated from room temperature to 100°C and maintained for 2 min to remove moisture and then quenched at −50°C for measurements.

The optical transmittance (T_r) of the PUBA films with 200 μm thickness were measured with an ultraviolet–visible spectrophotometer (UV-160A, Shimadzu, Japan) at a wavelength of 800 nm. Tensile strength and elongation at break of the films were measured on a universal testing machine (CMT 6503, Shenzhen SANS Test Machine China) with a strain rate of 50 mm min^{-1}. According to ISO 527-3-1995 (E), an average value of at least five replicates for each sample was obtained.

Swelling test

The crosslink density of the various PUBA and PU films was determined according to the swelling tests reported by Yoshida et al.[22] Before testing, the PUBA films were extracted with acetone to remove the soluble material. Three film samples having weights of ~0.2 g each were placed into toluene and allowed to stand for 5 days at 25°C. After achieving swelling equilibrium, the resulting samples were removed from the toluene and weighed after removing the excess toluene. The crosslink density of the PUBA films was obtained by using the following equation:

$$\frac{v_c}{V_0}(\mathrm{mol/cm^3}) = \frac{-2\left[\upsilon + \chi\upsilon^2 + \ln(1-\upsilon)\right]}{\mathrm{V}_1(2\upsilon^{1/3} - \upsilon)} \tag{3}$$

where ν_c = effective molar number of cross linked chains, V_1 = molar volume of solvent, χ = polymer–solvent interaction parameter, υ = volume fraction of dry polymer in swollen gel ($\upsilon = V_0/V$), V_0 = volume of dry polymer, V = volume of swollen gel at equilibrium. To determine χ of the PUBA semi-IPN in toluene system, the swelling tests were performed at 27, 29, 32, and 36°C. From the temperature dependency of the swelling volume, χ values were obtained using the following:[23]

$$\frac{d\ \ln\upsilon}{d\ \ln T} = \frac{-3\chi(1-\upsilon)}{5(1-\chi)} \tag{4}$$

where T is temperature (K). χ values of the PUBA films were found to range from 0.34 to 0.38, so the mean value of 0.36 for the PUBA films was used to calculate the crosslink density. The density of the PUBA films at 27, 29, 32 and 36°C was measured by determining the weight of a volume calibrated pycnometer filled with a mixture of NaCl aqueous solution and distilled water in which the sample achieved a specific floatation level.

RESULTS AND DISCUSSION

Molecular weight and chain conformation of BA

The ^{1}H NMR and ^{13}C NMR spectra of BA0 are shown in Figure 1. They were recorded on an INOVA-600 spectrometer (Varian) in DMSO-d_6 at

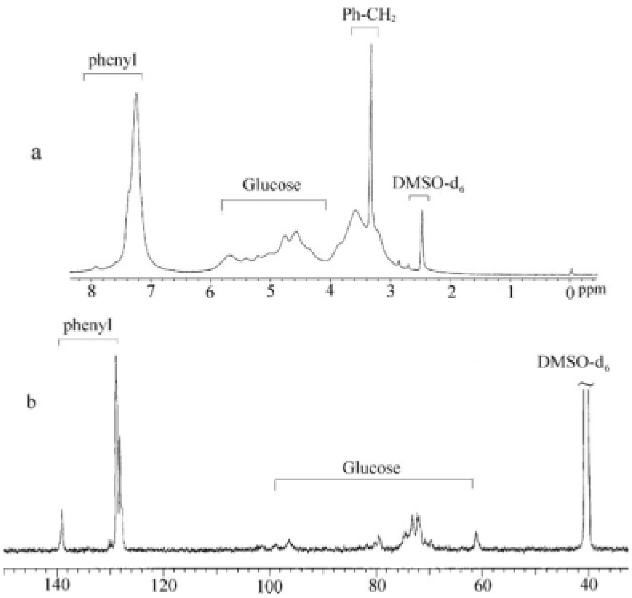

Figure 1 ^{1}H NMR (a) and ^{13}C NMR (b) spectra of BA0.

room temperature in which the concentration of BA was 5 wt %. From Figure 1(a), it can be seen that the main peaks appeared at 7.25 ppm (H of phenyl) and 3.3 ppm (H of methylene in benzyl), which indicated that the substitution was successful. The ^{13}C NMR spectrum of BA0 shows a characteristic chemical shift of phenyl groups that ranged from 128 to 139 ppm; the signal of 139 ppm can be assigned to the carbon atom of phenyl group linked to $-CH_2-$. This result further confirms that specific hydroxyl groups were successfully substituted by benzyl groups.

A typical Zimm plot for BA3 in DMF at 25°C is shown in Figure 2. The M_w, $<S^2>_z^{1/2}$, [η], and DS values of the fractions are listed in Table I. When varying the DS of BA within a small range (0.94 to 1.05), any effect on the chain conformation cannot be observed. Therefore, the chain conformation parameters of BA can be estimated according to current polymer solution theories. The results indicate that M_w and $<S^2>_z^{1/2}$ values for BA decrease with an increase in the exposure time of amylose in sulfuric acid aqueous solution, in accordance with the degradation of their molecular chains. Figure 3 shows the double logarithmic plot of $<S^2>_z^{1/2}$ versus M_w for BA in DMF at 25°C. In the M_w range from 2.69 × 10^5 to 9.24 × 10^5, the plot of $<S^2>_z^{1/2}$ against M_w can be represented by:

TABLE I
The Experimental Data of M_w, $<S^2>_z^{1/2}$, and DS for BA

Samples	$M_w \times 10^{-5}$	$<S^2>_z^{1/2}$ (nm)	w_c (wt %)	DS
BA0	9.24	55.3	62.46	1.05
BA1	8.90	53.1	61.45	0.96
BA3	7.43	48.6	61.22	0.94
BA5	4.07	38.8	61.56	0.97
BA7	2.69	30.3	62.01	1.01

$$<S^2>_z^{1/2} = 0.097 \times M_w^{0.46} (\text{nm}) \quad (5)$$

The exponent shown above (0.46) is related to the shape of the macromolecules and the nature of the solvent. Generally, this exponential value for a normal, flexible polymer is in the range from 0.5 to 0.6. And, the macromolecules can be deemed an Einstein sphere if the exponential value reaches 0.33. Therefore, a value of 0.46 suggests that the BA molecules are a relatively compact random coil in DMF.

The miscibility of the PUBA semi-IPN

The SEM images of cross-sections of the PUBA films are shown in Figure 4. The PUBA films exhibit a homogeneous and smooth structure, indicating a good and uniform dispersion of BA component in the matrix of PU with strong interfacial adhesion regardless

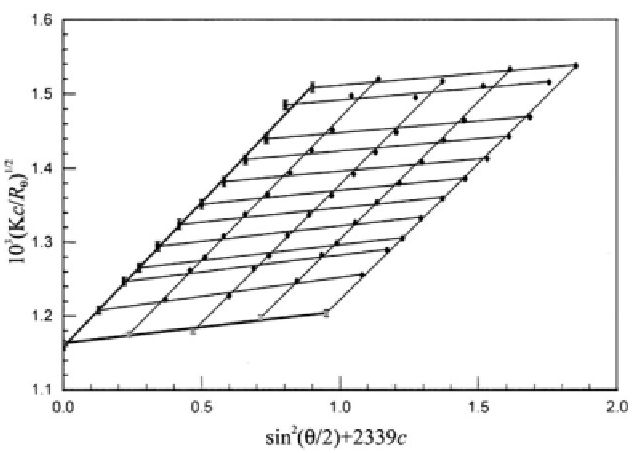

Figure 2 Zimm plot for BA3 in DMF at 25°C.

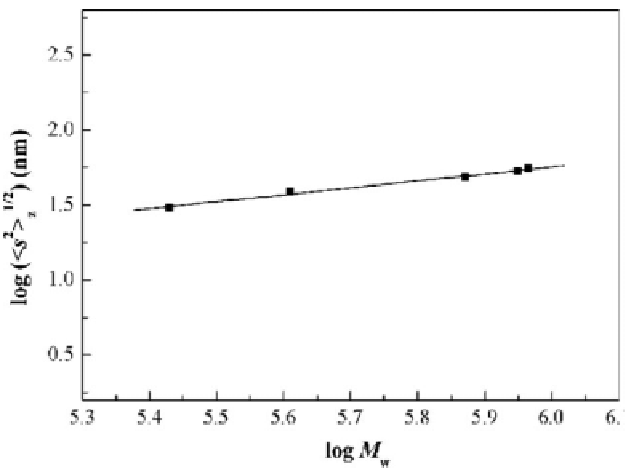

Figure 3 Double logarithmic plot of $<S^2>_z^{1/2}$ versus M_w for BA.

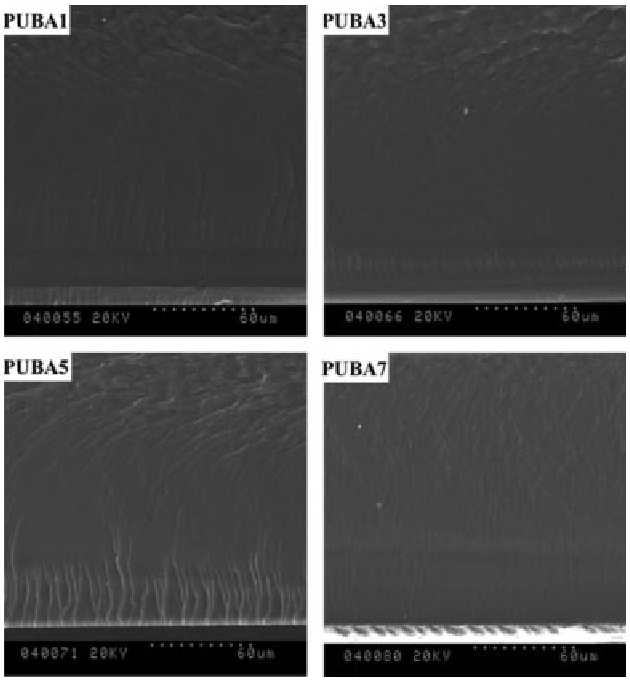

Figure 4 SEM images of the cross-sections of the PUBA films.

of the difference of M_w of BA. The reason for this may be the interactions of the π-electrons of the aromatic ring and the N—H hydrogen of the PU hard segments with the π orbital of the BA phenyl side groups.[24,25]

The dependence of crosslink densities (ν_c/V_0) of PUBA films on BA M_w is shown in Figure 5. Apparently, the cross link density of PUBA films is lower than that of the PU film. This indicates that the BA molecules in a compact random coil conformation can easily penetrate into a PU network and engage in strong interactions with PU molecules, which

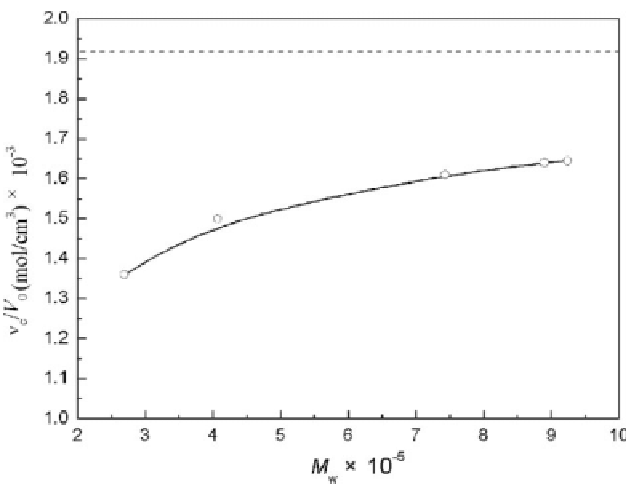

Figure 5 The dependence of crosslink density (ν_c/V_0) on BA M_w for the PUBA films. Dashed line represents the value of crosslink density of PU film.

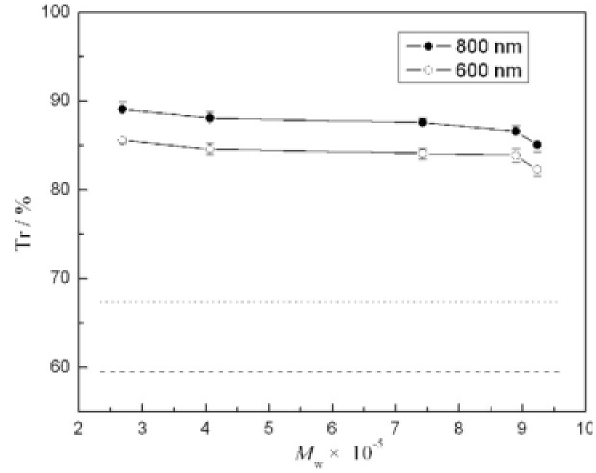

Figure 6 Effect of BA M_w on the optical transmittance (T_r) of the PUBA films at 600 and 800 nm. Dashed and dotted lines represent the T_r of the PU film at 600 and 800 nm, respectively.

results in an inhibition of PU network formation in the PUBA semi-IPN films. In addition, the crosslink density of PUBA films decreases from 1.65×10^3 to 1.36×10^3 mol/cm^3 with a decrease of M_w of BA from 9.24×10^5 to 2.69×10^5. This observation can be explained by the fact that the BA with a lower molecular weight more readily penetrates into the PU networks and more intimately blends with PU than the BA with a higher molecular weight.

The transparency of the films is often used as an additional criterion to judge the phase mixing in polymer composite materials.[26] The dependencies of

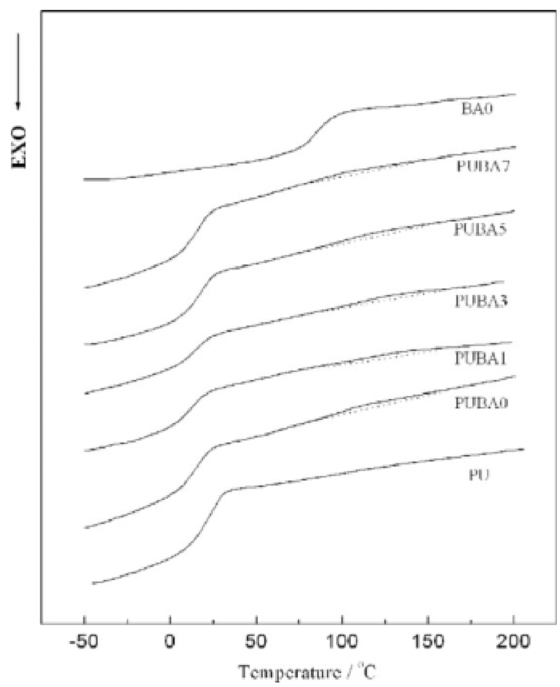

Figure 7 DSC thermograms of the BA0, PU, and PUBA films.

TABLE II
The Results from DSC of BA0, the PU and PUBA Films

Samples	PU	PUBA0	PUBA1	PUBA3	PUBA5	PUBA7	BA0
T_g (mid)/°C	20.3	14.6	12.1	17.6	15.4	17.2	105.0
ΔC_p/Jg^{-1} K^{-1}	0.46	0.36	0.26	0.23	0.34	0.37	0.29

T_r at 600 and 800 nm on BA M_w for the PUBA films are shown in Figure 6. It can be seen that the T_r values of the PUBA films at both 600 and 800 nm are much higher than those of the pure PU film. In general, microphase separated systems can also appear transparent when the two components have similar refractive indices. However, the higher T_r of PUBA here may be ascribed to the high T_r value of the BA component, good phase mixing, and strong interfacial adhesion between BA and PU. Furthermore, the T_r values of the PUBA films increase slightly from 82.3 to 85.6% and from 85.9 to 89.1% at 600 and 800 nm, respectively, with a decrease of the BA M_w from 9.24×10^5 to 2.69×10^5, indicating that the BA with lower M_w may penetrate and be more easily homogeneously dispersed in the PU network. Therefore, the reduction of BA M_w can enhance the miscibility between BA and PU.

The DSC thermograms of the BA0, PU, and PUBA films are shown in Figure 7, and the corresponding data are summarized in Table II. In the DSC curves, the midpoint of the thermogram step is taken as the glass transition temperature (T_g), and those of BA0 and PU are 105.0 and 20.3°C, respectively. For the PUBA films, two glass transitions are detected, indicating that the semi-IPNs are immiscible. The distinct glass transition that is located at low temperature ranges from 0 to 50°C is attributed to the PU soft segments. In this case, the presence of BA can influence the values of T_g of PU soft segments in two opposite ways. First, the incorporation of the BA molecules can induce a decrease in the crosslink density of the PU network, which results in an enhancement of the flexibility and mobility of PU soft segments and a shift of T_g toward lower temperature. In the opposite way, the solid surface of BA phase can result in an increase in the T_g of the soft WPU segments indirectly by engaging in strong interactions within the interfacial area. Obviously, the chemical crosslinks between CNs and WPU have a larger influence on the soft segment T_g, which can be substantiated by a decrease in the values of T_g for the PUBA films, compared to WPU. However, no consistent T_g is observed in the PUBA semi-IPNs with different BA M_w due to these two competitive effects. The other weak glass transition that ranged from 80 to 150°C can be assigned to the BA component. However, the values of the corresponding heating capacity are small because there was only a 20 wt % BA component in the PUBA films.

Mechanical properties

Normally, when polymer pairs exist in two phases, the mechanical properties of the blend material are governed by the distribution of the respective polymers within the blend. In other words, the properties may be dominated by the higher volume polymer phase. Polymer-rich phases usually form the continuous matrix, whereas the secondary phase plays the role of a reinforcement agent within the matrix via stress transfer between interfaces. Obviously, BA exists in the PU matrix as a reinforcement phase in the PUBA films. Figure 8 shows the dependence of tensile strength (σ_b) and elongation at break (ε_b) on BA M_w of the PUBA films. The pure BA film is too brittle; thus, the mechanical data of σ_b and ε_b cannot be obtained. The σ_b values of the PUBA films are much higher than that of the pure PU film, showing a significant enhancement of σ_b for the PUBA films. This indicates that the addition of 20 wt % BA provides a strong interaction with the PU component and acts as a stress transfer point in the PU continuous phase. With a decrease of BA M_w, the σ_b values of the PUBA films (except PUBA0) slightly decrease from 19.7 to 16.7 MPa, which can be explained by a lower crosslink density for the PUBA films with a lower M_w BA. Meanwhile, the values of ε_b significantly increase from 135 to 236% with a decrease of the BA M_w from 9.24×10^5 to 2.69×10^5. It is worth noting that the high flexibility of PU can be retained after adding 20 wt

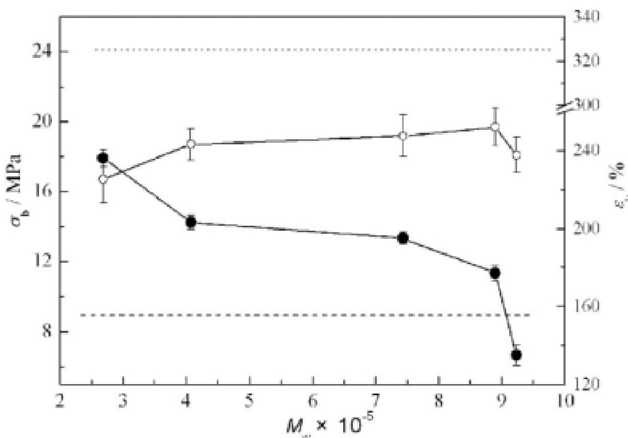

Figure 8 Dependence of tensile strength (σ_b, o) and elongation at break (ε_b, ●) of the PUBA films on BA M_w. Dashed (---) and dotted lines (L) represent tensile strength and elongation at break for the PU film, respectively.

% BA, especially when introducing BA that have low M_w. This latter result is due to a decrease in the crosslink density of the PU networks and an enhancement in the freedom of the molecular motion.

CONCLUSIONS

Based on current solution theories, the BA molecular chain conformation has been shown to be a relatively compact random coil in DMF. BA molecules are able to easily penetrate into the PU network to result in a large contact specific surface with strong adhesion. As a result, the PUBA films had much higher optical transmittance and tensile strength than PU films in the range of BA M_w that was used. Simultaneously, the high flexibility of the PU material was well retained. With a decrease in the BA M_w from 8.90×10^5 to 2.69×10^5, the crosslink density of PUBA films decreased from 1.65×10^3 to 1.36×10^3 mol/cm^3, which led to a significant increase in the elongation at break ranging from 135 to 236%.

The authors are indebted to a scholar exchange program between Wuhan University and NC State University that made portions of this work possible.

References

1. Yu, L.; Dean, K.; Li, L. Prog Polym Sci 2006, 31, 576.
2. Cao, X.; Chang, P. R.; Huneault, M. A. Carbohydr Polym 2008, 71, 119.
3. Cao, X.; Chen, Y.; Chang, P. R.; Stumborg, M.; Huneault, M. A. J Appl Polym Sci 2008, 109, 3804.
4. Chen, Y.; Cao, X.; Chang, P. R.; Huneault, M. A. Carbohydr Polym 2008, 73, 8.
5. Li, F.; Larock, R. C. Biomacromolecules 2003, 4, 1018.
6. Dufresne, A.; Vignon, M. R. Macromolecules 1998, 31, 2693.
7. Sugar, A. D.; Merrill, E. W. J Appl Polym Sci 1995, 58, 1647.
8. Suda, K.; Kanlaya, M.; Manit, S. Polymer 2002, 43, 3915.
9. Lu, Y.; Larock, R. C. Biomacromolecules 2007, 8, 3108.
10. Andjelkovic, D. D.; Larock, R. C. Biomacromolecules 2006, 7, 927.
11. Wang, H. J.; Rong, M. Z.; Zhang, M. Q.; Hu, J.; Chen, H. W.; Czigány, T. Biomacromolecules 2008, 9, 615.
12. Lligadas, G.; Ronda, J. C.; Galia, M.; Cadiz, V. Biomacromolecules 2006, 8, 686.
13. Zlatanic, A.; Petrovic, Z. S.; Dusek, K. Biomacromolecules 2002, 3, 1048.
14. Nevia, N.; Manson, J. A.; Sperling, L. H. Macromolecules 1979, 12, 360.
15. Zhang, L.; Zhou, Q. J Polym Sci Part B: Polym Phys 1999, 37, 1623.
16. Gao, S.; Zhang, L. Macromolecules 2001, 34, 2202.
17. Lu, Y.; Zhang, L. Polymer 2002, 43, 3979.
18. Lu, Y.; Zhang, L. Polymer 2003, 44, 6689.
19. Zhang, L.; Zhou, J.; Huang, J.; Gong, P.; Zhou, Q.; Zheng, L.; Du, Y. Ind Eng Chem Res 1998, 38, 4284.
20. Cao, X.; Zhang, L. J Polym Sci Part B: Polym Phys 2005, 43, 603.
21. Cao, X.; Zhang, L. Biomacromolecules 2005, 6, 671.
22. Yoshida, H.; Mörck, R.; Kringstad, K. P. J Appl Polym Sci 1987, 34, 1187.
23. Flory, P. G.; Rehner, J. J chem Phys 1943, 11, 521.
24. Theocaris, P. S.; Ketalas, V. J Appl Polym Sci 1991, 42, 3059.
25. Wang, F. C.; Feve, M.; Lam, T. M.; Pascault, J. P. J Polym Sci Part B: Polym Phys 1994, 32, 1315.
26. Weaver, K.; Stoffer, J. O.; Day, D. E. Polym Compos 1995, 16, 161.